

Instabilities & Turbulence

by *Didier Besnard,*
Francis H. Harlow,
Norman L. Johnson,
Rick Rauenzahn,
and *Jonathan Wolfe*

When the interface between two materials experiences strong accelerative or shearing forces, the inevitable results are instability, turbulence, and the mixing of materials, momentum, and energy. One of the most important and exciting breakthroughs in our understanding of these disruptive processes has been the recent discovery that the features of the processes often are *independent of the initial interface perturbations*. This discovery is so important that scientists at Los Alamos National Laboratory, the California Institute of Technology, the Atomic Weapons Research Establishment in Great Britain, Lawrence Livermore National Laboratory, as well as scientists in France, and no doubt in the Soviet Union, are working hard to confirm and extend this new understanding experimentally.

Theoretical analyses are likewise showing a firm basis for this astonishing discovery. Two types of theory are being employed, gradually combined, and even proved essentially equivalent. These are the *multifield-interpenetration approach* and the *single-field turbulence approach*. Even brute-force hydrodynamics calculations are demonstrating this same property of independence from initial perturbation.

The consequences for developments in such main-line Laboratory projects as inertial-confinement fusion are profound. Our entire view of material mixing, turbulence shear impedance, and energy transport has undergone a revolutionary shift to qualitatively different directions.

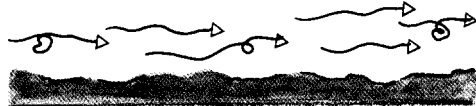
What is the physical essence of this new way of thinking? No matter how

TURBULENCE EFFECTS

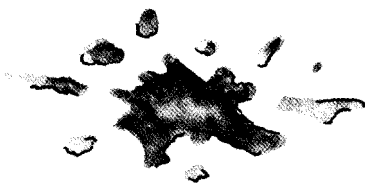
Fig. 1. The effects of turbulence include increased mixing of initially separated materials, an increase in shear impedance of fluid near rough boundaries due to the turbulent viscosity, and increased transport of heat into surrounding cooler regions.



Increased Mixing of Materials



Increased Shear Impedance



Increased Heat Diffusion

carefully we attempt to achieve smoothness and homogeneity, any sufficiently strong destabilizing influence at a material discontinuity will inevitably be disruptive. Indeed, the disruptive effects will be manifested in essentially the same manner as if there were a considerable roughness or inhomogeneity at or near the interface. Add to this the effects of any long-wavelength asymmetries, and we have an immutable inevitability for major instabilities in virtually every experimental circumstance of accelerative or shearing dynamics of interest to the Laboratory. Reliable predictability of new weapons designs in a comprehensive test ban, the design of any locally intense energy source, the development of workable concepts in Strategic Defense, the achievement of successful inertial-confinement fusion devices, and the success of many other Laboratory programs will depend crucially on our ability to model these instability and turbulence effects realistically.

What Is Turbulence?

To describe the techniques we are using to model these effects, we must first consider in more detail the properties of turbulence itself. Turbulence is the random fluctuation in fluid motion that often is superimposed on the average course of the flow. The effects of turbulence can be highly significant (Fig. 1), increasing the fluid's effective viscosity and enhancing the mixing of initially separated materials, such as the mixing of dust into air or bubbles into a liquid. Turbulence is a significant factor in the wind resistance of a vehicle, in the dispersal of fuel droplets in an internal combustion engine, in mixing and transporting materials in chemical plants, indeed in virtually every circumstance of high-speed fluid flow.

It is easy to be deceived into thinking that turbulence is rare, because it often is not directly visible to the casual observer. Although water flowing rapidly through a transparent pipe may look completely smooth, touching the pipe can reveal large vibrations and the injection of dye through a tiny hole in the wall can demonstrate rapid downstream mixing. Both effects are a direct result of intense turbulent fluctuations.

Turbulence in air can be demonstrated—even in a relatively calm room—by holding one end of a long thread and watching its fluctuating response to air currents. Sunshine streaming over the top of a hot radiator creates shadow patterns on a nearby wall that dance restlessly in the never-ending turbulence that accompanies the upward flow of air.

Why is nature discontent with the smooth and peaceful flow of liquids and gases, especially at high flow speeds? What are the processes that feed energy into turbulent fluctuations? The answers lie in the behavior of energy. In contrast to momentum, energy has the peculiar ability to assume numerous and varied configurations. Momentum constraints, while restrictive, are helpless to prevent seemingly capricious energy rearrangements. In any real fluid flow, these rearrangements are triggered by inevitable perturbations that can be fed from the reservoir of mean-flow energy.

It is helpful at this point to compare turbulence with the random motion of simple gas molecules in a box because the approaches to both of these problems include much that is similar. However, the analogy becomes seriously misleading if pushed too far.

Molecular Systems. In a box of molecules the dynamics of each individual can

be described quite accurately by Newton's laws. Yet we seldom try to analyze the complex interactions of all the trajectories, which are seemingly capable of very chaotic behavior. Instead, we appeal to the remarkably organized *mean* properties of the motion, identifying such useful variables as density, pressure, temperature, and fluid velocity.

We cannot ignore the departure of the individual from the behavior of the mean; indeed, some of the most interesting properties of the gas are directly associated with these departures. Diffusion of heat energy, for example, represents transport of kinetic energy by fluctuations; pressure in a "stationary" gas is the result of continual bombardment of molecules against objects immersed in the gas (Fig. 2(a)); viscous drag between two opposing streams of gas (Fig. 2(b)) arises because of fluctuations from the mean-flow velocity that cause molecules to migrate from one stream to the other.

Turbulent Eddies and Mean Flow. Turbulent eddies in a fluid superficially resemble individual molecules in a gas. They likewise bounce around in random fashion, carrying kinetic energy in their fluctuational velocities. (Such turbulence kinetic energy is typically as much as 10 per cent of the mean-flow kinetic energy, or even more in regions where the mean flow stagnates at a solid surface.) Eddies also diffuse momentum (plus heat and any imbedded materials), exerting pressure through momentum transport and bombardment against walls.

But the concept of a turbulent eddy is nebulous at best. Gas molecules have an easily identifiable shape, size, mean separation, and mean free path between collisions. Turbulent eddies, in contrast, have a spectrum of sizes; they overlap each other; the constraint on their motion through the fluid by the immediate presence of neighboring fluid precludes the simple concept of a mean free path.

Moreover, identification of what part of the dynamics is turbulence and what part is mean flow is arbitrary. For molecules the distinction is essentially unique; in most circumstances, individual molecular fluctuations take place on a scale that is orders of magnitude smaller than the scale of collective, fluid-like motion. For turbulent eddies the fluctuational scale may be an appreciable fraction of the mean-flow scale. More to the point, the observer's experimental configuration itself establishes the distinction between turbulence and mean flow.

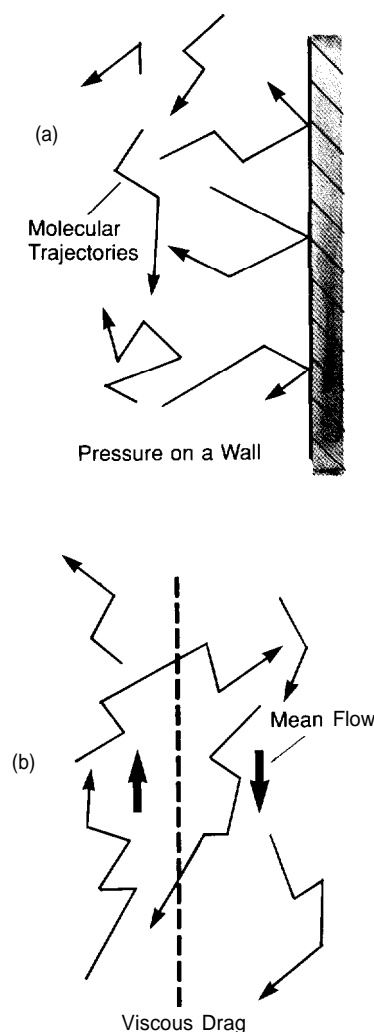
To put the matter succinctly, mean flow is that part of the dynamics directly associated with the macroscopic conditions established or measured by the **observer**, whereas turbulence is the more capricious part of the flow associated with finer-scaled perturbations not controlled by the observer but inevitably present in any real flow.

As an example, consider air flow around a parked automobile on a gusty day. With suitable instruments an observer can record variations in the approaching wind velocity. These measurements describe the source of the mean flow, and the macroscopic features of the car constitute the boundary conditions. Mean-flow patterns in the wake on the downwind side of the vehicle can be observed either with a ribbon that stretches out with the average air velocity at each place it is held or with an upstream smoke generator emitting a thin filament of smoke that can be photographed as it passes over the car.

Both the ribbon and the filament have an *average* direction to their motion that varies on the same time scale as that of the monitored gusts of wind; the relationship between these two features is the correlation that our investigator is seeking. In addition,

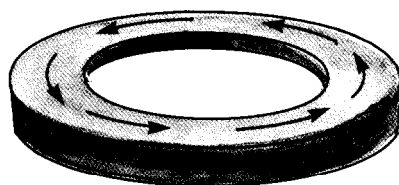
MOMENTUM FLUX

Fig. 2. (a) The pressure on a wall is the result of the transfer of momentum during collisions between individual molecules and the wall. (b) Viscous drag between two opposing streams of gas is a result of individual departures from the mean-flow velocity in each stream. More precisely, pressure and viscous drag represent the normal flux through any imaginary surface of the normal and the tangential components of momentum, respectively.



TANGENTIAL DRAG

Fig. 3. Fluid moving in a circular trough loses mean-flow kinetic energy because of tangential drag on the walls. Although this entire loss in energy will eventually appear as heat, a significant fraction may first appear as the kinetic energy of turbulence.



however, the ribbon flutters rapidly about that average (at the rate of many fluctuations per second), and the smoke filament diffuses in contorted kinks into the surrounding air. This capricious variation around the time-varying average is what our observer calls turbulence.

A second observer standing nearby, but paying no attention to the detailed observations of the first, feels buffeted by the gusts and, likewise, would agree that there is much turbulence. However, this observer can legitimately disagree as to which part of the air flow is mean flow and which part is turbulence, seeing an average southwesterly wind with turbulent variations that last several seconds. Meanwhile, an earth-orbiting satellite reveals that the southwesterly wind is simply a momentary fluctuation (of a half hour or so) from the general westerlies crossing the continent that day.

This example has three different fluctuational scales, all properly identified as turbulence on the basis of the observer's chosen viewpoint. The difference, however, is not merely one of semantics, and we discuss below the consequences of this multiple viewpoint to mathematical modeling of the flow processes. Important guidance is furnished by a careful consideration of interactions among the various dynamical scales.

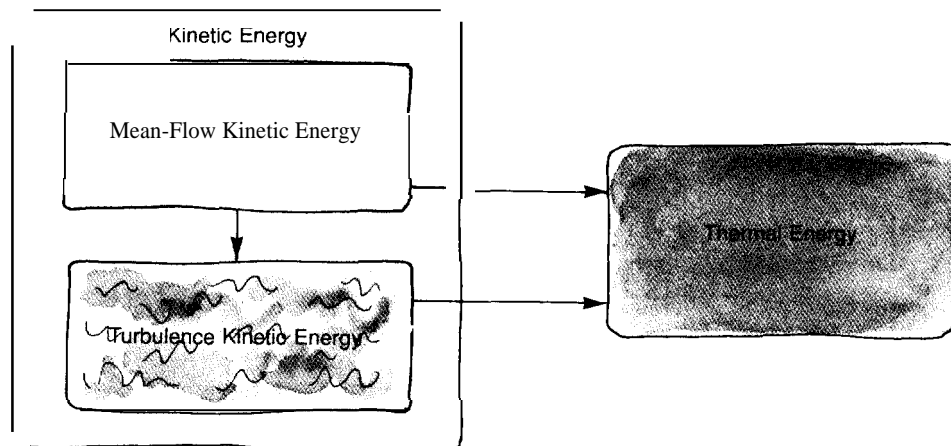
There is thus a seemingly random nature to both molecular dynamics and turbulence. The detailed flow field of a group of molecules or eddies can vary by large amounts as a result of minor initial perturbations on a microscopic scale. But the remarkable feature of these dynamical systems is that the overall stochastic behavior is essentially independent of the manner in which the fluctuations are introduced.

However, not every fluid flow is sensitive to minor perturbations. Viscous or *slowly* moving fluids travel in a purely laminar fashion, responding negligibly to fine-scale perturbations. Why does flow remain stable for some conditions and exhibit turbulence for others? The answer lies in the ways in which energy is drawn from the mean flow as the motion gradually decays to quiescence.

Turbulence Energy: Sources and Sinks

The statements of mass, momentum, and energy conservation lie at the foundations of fluid dynamics. In particular, fluid flow implies the presence of energy, which can exist in any of various forms: kinetic, heat, turbulence, potential, chemical. For the moment we are concerned only with the first three. By kinetic energy we mean the motion energy carried by the *mean flow*; heat energy refers to the kinetic energy of *molecular* fluctuations. Turbulence energy is at a scale between these first two: it is the kinetic energy of fluctuations that are large compared with the individual molecular scale but small compared with the mean-flow scale.

As we said earlier, in contrast to mass and momentum, which are highly constrained by their conservation laws, energy behaves very capriciously. Although *total* energy is rigorously conserved, transitions among the many manifestations of energy occur continuously. It is a remarkable fact of nature that, as a result of such transitions, any system devoid of remedial influences inevitably tends to move from order to disorder. An egg hitting the floor turns to a mess as ordered kinetic energy is converted into splat. Cars break down, rust, and eventually end up as nondescript piles of metallic and organic compounds blowing in the wind or leached by groundwater into a progressively wider and less ordered distribution. Fluids in a nicely ordered state of mean flow likewise



ENERGY DEGRADATION

Fig. 4. The mean-flow kinetic energy of a moving fluid inevitably degrades to thermal energy. Frequently, however, part of that kinetic energy is first transformed to kinetic energy of turbulence.

tend toward (mass- and momentum-conserving) states of disordered energy in which the only residuum is heat—and even that leaks off to the less ordered state of wide dispersal as a result of conduction and radiation. In thermodynamics, the trend from order to disorder is called the Second Law; its profound scientific and philosophical implications have been discussed and debated for many decades; its validity is beyond doubt.

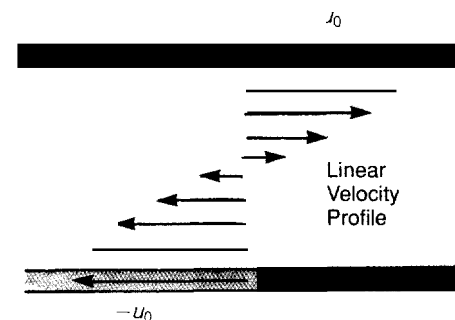
Consider a fluid that has been set into smooth and uniform motion in a circular trough (Fig. 3). It has zero total (vector) momentum: as much is moving east as is moving west at every instant. Tangential shearing drag on the walls slows the motion so that mean-flow kinetic energy is lost. Where does the energy go—to turbulence or to heat? The competition is fierce, and heat always wins in the end, but fluids yield themselves to the inevitable only grudgingly. If at all possible, they transform at least part of their kinetic energy to turbulence as an intermediate step along the way (Fig. 4).

Let's replace this animistic description with physics. The conversion of mean-flow kinetic energy directly to heat is limited by the viscosity of the fluid and by the steepness of the mean-flow velocity gradients. For example, consider fluid flow between two plates moving in parallel but opposite directions (Fig. 5). Although a variety of flow-velocity profiles could have been depicted, the one shown has the smallest fluid kinetic energy of any flow profile with that same momentum between the moving plates. This profile is thus the flow distribution to which all others inevitably tend.

Suppose we now examine a flow profile at the opposite extreme—one in which the gradient at the midpoint between the plates is very sharp (Fig. 6(a)). Both this distribution and the stable one in Fig. 5 have the same total fluid momentum (namely zero); however, in the distribution in Fig. 6(a), every fluid element has the same speed (u_0), whereas in the stable distribution, most elements are moving slower than u_0 . Thus the fluid in Fig. 6(a) possesses an excess of kinetic energy compared to the fluid with the stable profile and will lose part of this energy as it transforms toward the stable configuration. Will turbulence be an intermediate state in this evolution? To answer this question we must dig deeply into the competitive processes of dissipation and instability.

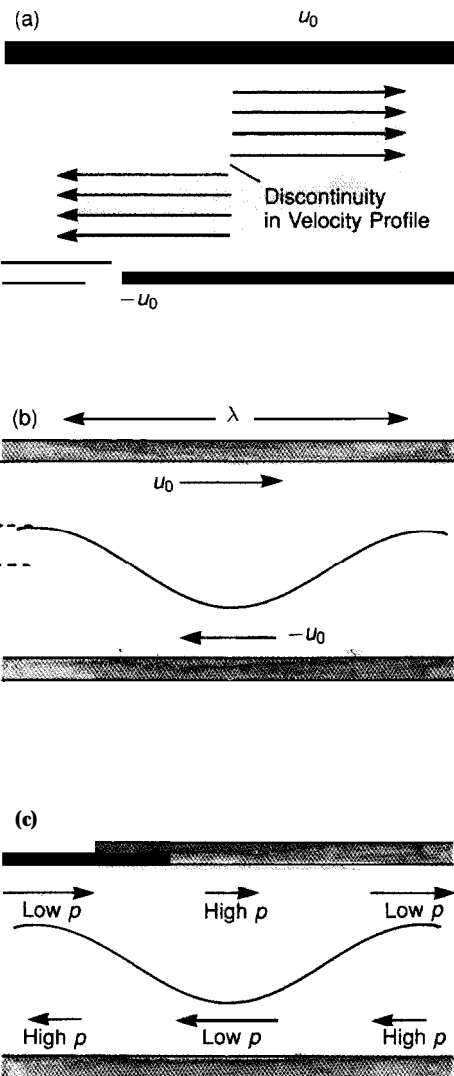
STABLE FLOW BETWEEN MOVING PLATES

Fig. 5. When fluid is trapped between two plates moving at speed u_0 in parallel but opposite directions, a gradient in fluid velocity is established. The linear flow-velocity profile shown here has the smallest kinetic energy of any profile at that same total momentum for the given boundary conditions.



UNSTABLE FLOW

Fig. 6. A discontinuity in the velocity profile between two oppositely moving fluid regions can lead to a Kelvin-Helmholtz instability at that interface, resulting in turbulence. For example, if, as in (b), the interface experiences a sinusoidal perturbation of wavelength λ and amplitude A , such a perturbation will act effectively as a series of Venturi nozzles (c) that alter the mean-flow velocities and pressure p . These pressure variations, in turn, further increase the distortion.



Consider first the dissipation of mean-flow kinetic energy into heat. Let H be heat energy per unit volume and du/dy describe some measure of the mean-flow velocity gradient in a fluid with molecular viscosity μ_m . Then the rate at which heat is generated is given by

$$\frac{dH}{dt} = \mu_m \left(\frac{du}{dy} \right)^2 \tag{1}$$

To estimate the rate at which turbulence energy is generated, we return to the flow described in Fig. 6(a), which is susceptible to a destabilizing process called the Kelvin-Helmholtz instability. The presence of such an instability is easily demonstrated for an incompressible fluid if we arbitrarily assume that the slip interface between the upper and lower halves of the flow profile is distorted by a sinusoidal wave of wavelength λ and amplitude A (Fig. 6(b)). Because the fluid is incompressible, wherever the flow area is constricted the fluid has to move faster than average, and wherever the flow area is expanded the fluid has to move more slowly (Fig. 6(c)). What is the associated behavior of the pressure? Each cycle in the perturbation is like a Venturi nozzle, for which Bernoulli's law says the pressure is less in the constricted region where fluid speed is higher and is greater in the expanded region where fluid speed is lower. Thus, there is a pressure difference across the perturbed slip plane, acting in *exactly the right direction to enhance the perturbation amplitude*.

More formally, we can associate an appropriate inertia with the material being accelerated (the acceleration of the perturbation in the slip plane is d^2A/dt^2), and we can use Bernoulli's law to calculate the pressure difference (the driving force for enhancing the perturbation), which is proportional to the square of the fluid speed u_0^2 . Newton's second law then leads to the following formula for the behavior of the perturbed slip plane:

$$\frac{d^2A}{dt^2} = \left(\frac{2\pi u_0}{\lambda} \right)^2 A \tag{2}$$

The growth in amplitude is dA/dt , so the kinetic energy per unit volume involved in this turbulent-like motion is

$$K \approx \frac{1}{2} \rho \left(\frac{dA}{dt} \right)^2 \tag{3}$$

where ρ is the density of the fluid. Differentiating Eq. 3 and substituting Eq. 2, we see that turbulence energy K , in turn, grows as

$$\frac{dK}{dt} \approx \left(\frac{2\pi u_0}{\lambda} \right)^2 \rho A \frac{dA}{dt} \tag{4}$$

With $\omega \equiv (2\pi u_0/\lambda)$, a solution of Eq. 2 is $A = A_0 e^{\omega t}$, and

$$\frac{dK}{dt} \approx \omega^3 \rho A_0^2 e^{2\omega t} \tag{5}$$

or

$$\frac{dK}{dt} \approx 2\omega K \tag{6}$$

The essence of these results is that dK/dt increases with time (ω is positive), whereas, because viscosity smears out the sharp velocity transition, thus decreasing du/dy , dH/dt decreases with time (Eq. 1). Whenever the amplitude (scale) of the disturbance is large enough, turbulence creation will dominate.

The important dimensionless quantities involved in the competition between turbulence energy creation and heat dissipation can be illustrated by taking the ratio of the growth rates of turbulence energy and heat energy at $t = 0$. Using Eqs. 1 and 6 and setting $du/dy \approx 2u_0/A$ at $t = 0$ we find

$$\left(\frac{dK/dt}{dH/dt} \right)_{t=0} \approx 2\pi^3 \frac{u_0 \rho A_0}{\mu_m} \left(\frac{A_0}{\lambda} \right)^3, \quad (7)$$

Local Initial
Reynolds Pertur-
Number bation

where A_0/λ can be thought of as a measure of the extent of the initial perturbation. The appearance in this equation of the local Reynolds number is not surprising, given that the number is a measure of the competition between the inertial and viscous effects in any flow (see "Reynolds Number").

As long as dH/dt dominates, the mean-flow kinetic energy dissipates to heat, and the intermediate turbulent stage is bypassed; we say that the mean flow is stable. If dK/dt dominates, then the mechanism driving the instability draws the excess kinetic energy into turbulence. We can thus formulate a stability criterion, based on the Reynolds number, in which molecular viscosity plays a central role. For large viscosity, dH/dt is able to exactly balance the loss rate for mean-flow kinetic energy. Decreasing the viscosity eventually drops dH/dt below the mean-flow loss rate, and the flow becomes unstable.

As a corollary, note that conservation of *total* energy raises an interesting question about mean-flow dynamics. What mechanism accounts for destruction of mean-flow kinetic energy at exactly the required rate to ensure conservation? The answer is viscosity—molecular viscosity and *turbulence* viscosity.

For the case of *only* direct viscous dissipation to heat, viscous drag between the opposing currents causes each to slow down, and the corresponding loss rate for kinetic energy exactly accounts for the dissipative heating. For the case of transfer of mean-flow kinetic energy to turbulence, a directly analogous process occurs in which turbulence viscosity produces drag. More precisely, the presence of turbulence induces a fluid shear stress, the Reynolds stress, that is independent of the molecular viscosity of the fluid. Expression of the components of the Reynolds stress tensor in terms of readily measured flow quantities (such as pressure and mean-flow velocity) lies at the heart of our theoretical work and is discussed in detail in the next section.

Analogous to molecular viscosity, turbulence viscosity depletes mean-flow kinetic energy at precisely the same rate that turbulence energy is growing. A direct consequence is that turbulence contributes to the effective viscosity of the fluid, enhancing the rate of momentum diffusion from one part of the fluid to another as it simultaneously destroys the excess mean-flow kinetic energy. As we shall see, turbulence diffuses *anything* imbedded in the fluid—momentum, heat, dye, dust particles, dissolved salts.

Reynolds Number

T design and test proposed large-scale equipment, such as airfoils or entire aircraft, it is often much more practical to experiment with scaled-down versions. If such tests are to be successful, however, dynamic similitude must exist between model and field equipment, which, in turn, implies that geometric, inertial, and kinematic similitude must exist.

The Navier-Stokes equations (Eqs. 9 and 10 in the main text) are a good starting point for deriving the relationships needed to establish dynamic similitude. First, we look at the case of laminar flow. Ignoring body force and pressure effects, we examine the momentum conservation relationship for steady, laminar, incompressible, two-dimensional flow, equating just the advection and diffusion terms in the x-direction:

$$\underbrace{\frac{\partial uu}{\partial x}}_{\text{Advection}} + \underbrace{\frac{\partial vu}{\partial y}}_{\text{Diffusion}} = \nu_m \left[\frac{d^2u}{dx^2} + \frac{d^2u}{dy^2} \right]. \quad (1)$$

Here u and v are the x and y components of the velocity and ν_m is the molecular kinematic viscosity (the ratio of fluid viscosity to fluid density μ_m/ρ). Advection has to do with kinematic effects, that is, the transport of fluid properties by the motion of the fluid, and thus accounts for momentum transport *along* streamlines; the diffusion terms represent viscous effects that cause momentum to diffuse *between* streamlines, thereby tending to di-

minish any sharp velocity gradients.

We can write Eq. 1 in dimensionless form by introducing a length scale L and a fluid velocity in the free stream u_0 . The result is

$$u_0 \left[\frac{\partial uu}{\partial x} + \frac{\partial vu}{\partial y} \right] = \frac{\nu_m}{L} \left[\frac{d^2u}{dx^2} + \frac{d^2u}{dy^2} \right], \quad (2)$$

where the highlighted variables are dimensionless. This portion of the momentum equation can thus be uniquely characterized by the ratio of the coefficients multiplying the dimensionless advection and diffusion terms. The ratio, called the Reynolds number

$$R = \frac{u_0 L}{\nu_m}, \quad (3)$$

can be thought of as a comparative measure of inertial and viscous (diffusive) effects within the flow field. To achieve dynamic similitude in two different laminar-flow situations, the Reynolds numbers for both must be identical.

What happens if we increase the flow speed to the point that viscous dissipation can no longer stabilize the flow, and the macroscopic balance between mean-flow inertia and viscous effects breaks down? At this point there is a transition from purely laminar flow to turbulence. In similar flows, the transition occurs at a specific Reynolds number characteristic of the flow geometry. For instance, any fluid traveling inside a circular pipe—regardless of the specific fluid or conduit

being used—experiences the onset of turbulence at $R \cong 2000$.

At or near this “critical” Reynolds number, inertial contributions to mean-flow momentum that cannot be dissipated by viscous stresses must be absorbed by newly formed turbulent eddies. The presence of turbulence energy is often described in terms of an effective turbulence viscosity ν_t , defined as the ratio of the turbulence-shear, or Reynolds, stress to the mean-flow strain rate. With this in mind, an effective *turbulence* Reynolds number—one that includes molecular viscous effects—is

$$R_{\text{eff}} = \frac{u_0 L}{\nu_t + \nu_m} \quad (4)$$

Molecular viscous effects are overwhelmed if $\nu_t \gg \nu_m$. In those instances the exact value of the kinematic viscosity ν_m is immaterial, and flow behavior is dominated by turbulence effects.

Although a turbulence Reynolds number may be entirely adequate for research on macroscopic flows, the analysis of turbulence *substructure* requires a third Reynolds number, a local turbulence Reynolds number based not on L and u_0 but on representative eddy size s and eddy velocity u' :

$$R_s = \frac{u' s}{\nu_m}. \quad (5)$$

Note that the molecular kinematic viscosity ν_m is retained in this definition. The choice of molecular viscosity to characterize the dissipative mechanisms responsible for tearing eddies apart is based on the ultimate transformation of turbulence into heat energy. Molecular processes are, in the end, dominant at the smallest scales, and R_s is a relative measure of the loss of kinetic energy from an eddy of a given size to heat. For the smallest eddies in a flow system, $R_s \cong 1$; that is, all the energy of the eddy is dissipated into heat. ■

What then can we deduce from this example about the features necessary for the creation of turbulence?

- A mean-flow profile richer in kinetic energy than other momentum-conserving states to which it can transform (such as the profile in Fig. 6(a) that can transform to the one in Fig. 5).
- A viscosity low enough that dissipation to heat cannot absorb all the mean-flow energy during the transition to the low-energy profile.
- A driving mechanism for enhancement of the inevitable microscopic perturbations (such as the Kelvin-Helmholtz instability in Fig. 6).

However, the energy of turbulence frequently comes from sources (Fig. 7) other than a velocity profile rich in mean-flow kinetic energy. For example, turbulence can be fed directly from potential energy as when a Rayleigh-Taylor instability develops at the interface between, say, water overlying a less dense layer of oil or cold air overlying warm air. The latter instance, called buoyancy-driven turbulence, produces the dancing air currents that can be seen by looking across the surface of a sunlit roof on a cold day. Similarly, turbulence can be fed by accelerative forces as when a Richtmyer-Meshkov instability develops at the deformable interface between two materials that are perturbed by, say, a passing shock wave or the sudden acceleration of the entire system.

Droplets, particles, or bubbles projected through a liquid or gaseous fluid with some relative velocity likewise can serve as a good source of turbulence energy. The momentum-conserving transition induced by drag tends always to bring such entities and the fluid to the same velocity. Competition for the center-of-mass kinetic energy results in a partition into both heat and turbulence—the winner again depending on the level of viscosity.

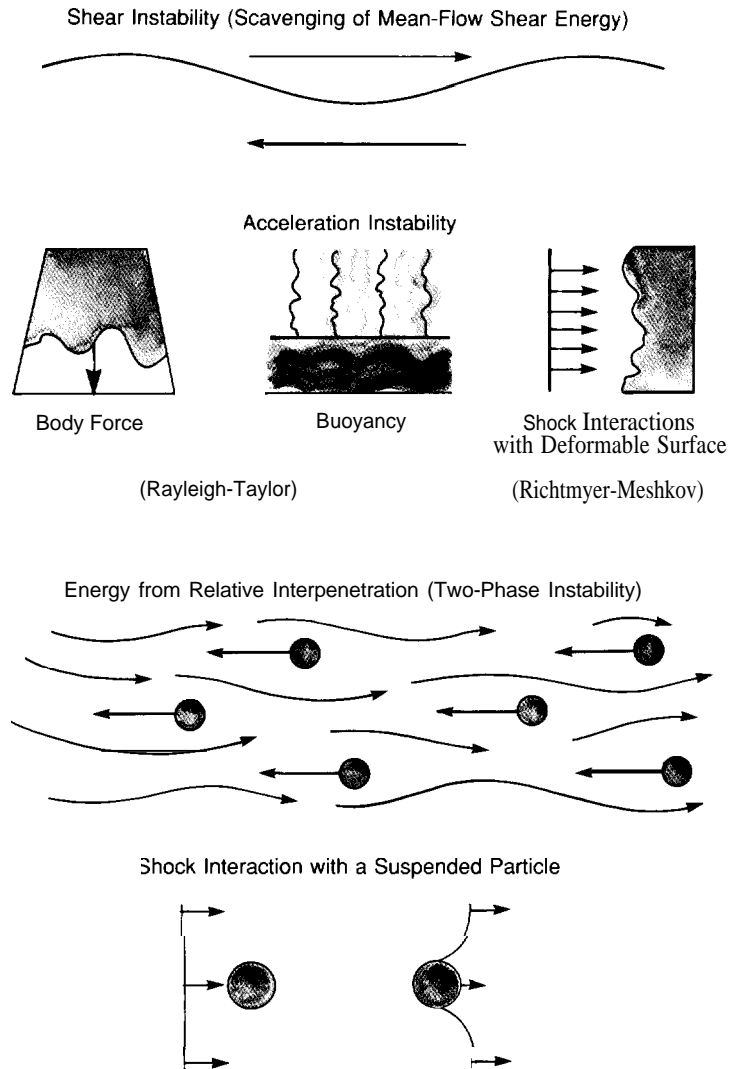
Likewise, if a quiescent suspension is subjected to a pressure gradient or shock, a differential acceleration occurs that is in proportion to the difference in densities between the suspended entities and the surrounding medium. Turbulence often gleans a significant share of the resulting interpenetrational energy.

Turbulence Sinks. So far we have been discussing only *sources* for turbulence and the manner in which the turbulence *decays*. Here we must return to what constitutes turbulence and, in particular, reaffirm that the existence of turbulence depends on the observer's point of view. Mean flow is that part of the dynamics whose structure is comparable in size to the region being measured; it is capable of being reproducibly duplicated or monitored—at least in some statistical sense. Finer dynamical scales of a capricious nature arising from random initial, boundary, or bulk perturbations constitute the fluid's turbulence. But the mean flow for one observer may simply be the larger scales of a turbulence spectrum for an observer whose field of view encompasses a somewhat larger domain. Thus, the *source* of turbulence seen by one observer becomes the energy *sink* for the decay of turbulence at the larger scales of another observer.

This principle and its generalizations have powerful consequences for our mathematical modeling of turbulence dynamics, leading to the concept of a *turbulence cascade*. In this process turbulence energy is transferred to progressively smaller and smaller fluctuational scales with the source of energy for each scale coming from the mean-flow velocity contortions of the next larger scale (Fig. 8). At each stage, there is competition for the energy, part going into heat and part going into even smaller

SOURCES OF TURBULENCE

Fig. 7. Although we have so far dealt only with shear instabilities (Figs. 5 and 6), there are many other sources of turbulence, ranging from the instability of one fluid overlying a less dense one, through the interpenetration of two distinct phases, to the interaction of a shock wave with particles or surfaces.



turbulent fluctuations. However, as the scale decreases, the characteristic length of the eddies decreases, and the velocity gradients in the eddies become steeper and steeper. In other words, dH/dt eventually wins, and, at the smallest of turbulence scales, energy goes directly to heat.

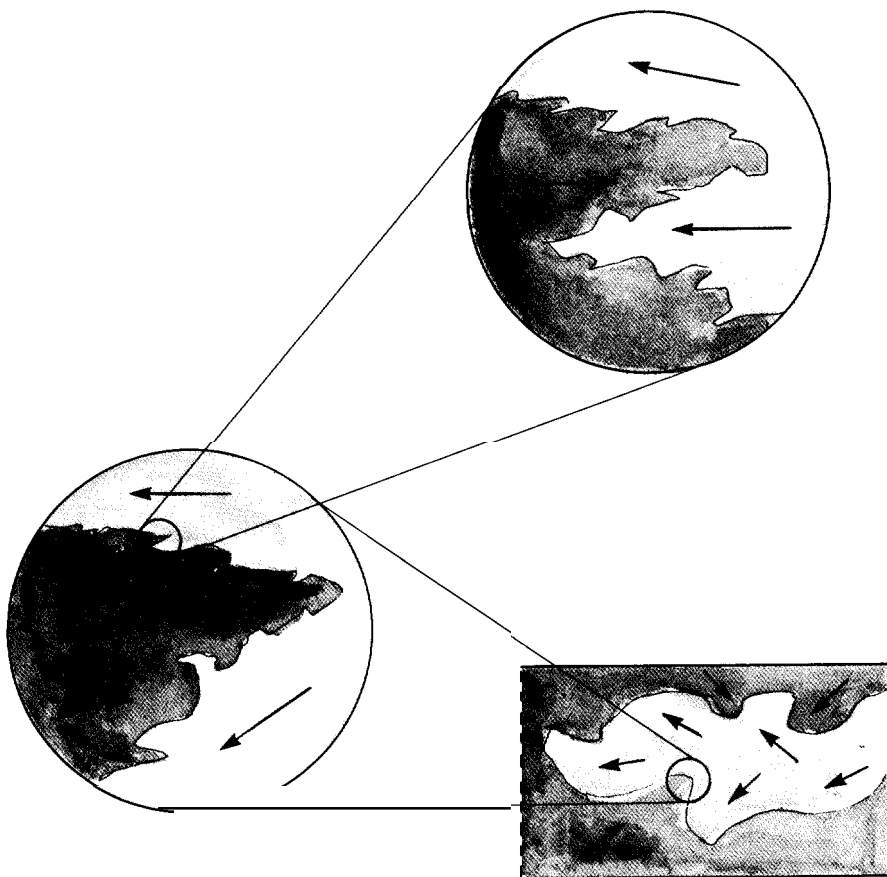
Thus, cascading of turbulence is consistent with nature's universal law dictating that ordered motion must become progressively more disordered until the energy in a flow degrades to heat. The direction and magnitude of energy flow within the cascade guides us in mathematically describing the decay of turbulence, not only into heat from very small-scale eddies but also from large scales to smaller scales. Because the transfer of energy through the cascade is, in some sense, equal at all steps, we can easily describe the energy decay rate in a manner independent of molecular processes. We will describe this approach more extensively when we consider detailed modeling

in the next section.

In an idealized steady-state approximation of turbulence, exactly as much energy enters the fluctuational spectrum of motion at the largest scale as leaves it to become heat at the smallest scale. More accurately, there is *some* loss of energy to heat at every scale, but the loss at the smallest scale is dominant (Fig. 9). Although these ideas have been exploited to derive interesting properties of the small-scale spectrum of turbulence energy, our principal concern here is with the largest scales. It is these scales that contain most of the energy and thus exert the dominant effects on mean-flow dynamics.

Transport Modeling of Turbulence

There are numerous theoretical approaches to turbulence: some reach to the conceptual heart of the matter, others are directed toward the solution of practical problems, and a few attempt to cover the entire range. Despite its present shortcomings, *turbulence transport theory*, which fits into the last category, already shows promise of considerable success in both illuminating the fundamental dynamical processes and serving as a vehicle for the solution of practical problems.

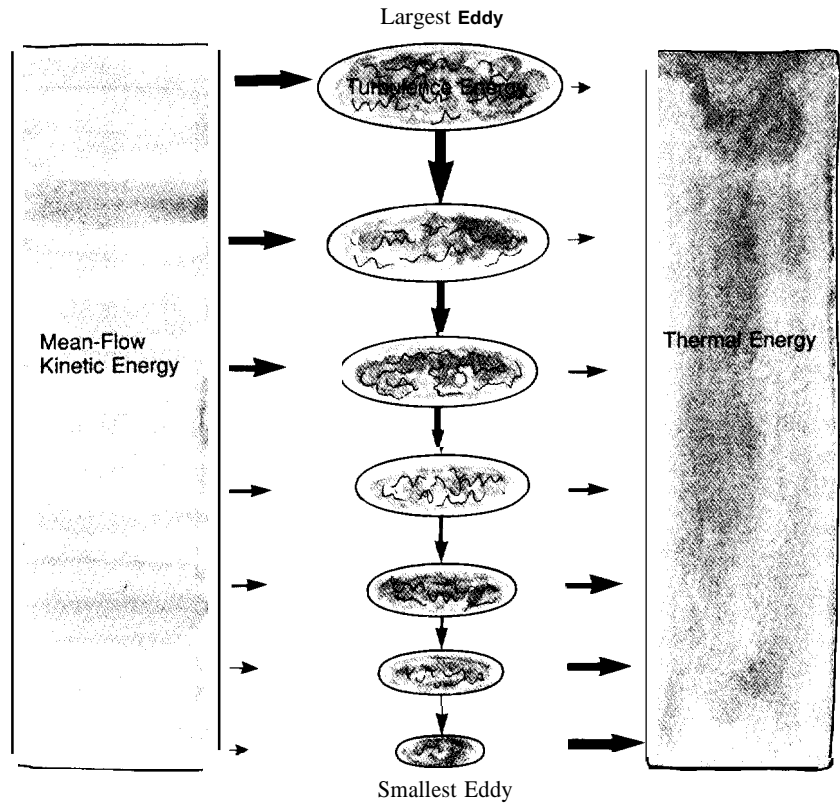


TURBULENCE CASCADE

Fig. 8. With each reduction in scale, turbulent motion of the larger scale becomes mean-flow motion of the smaller scale (arrows). Because each reduction in scale has approximately the same change in mean-flow velocity occurring over a much smaller distance, velocity gradients become steeper, and a larger fraction of the turbulence energy goes directly into heat.

TURBULENCE ENERGY FLOW

Fig. 9. Mean-flow kinetic energy transforms into turbulence energy and thence to heat energy, but the relative amounts (indicated by the sizes of the arrows) transported by each mechanism changes as the scale of the turbulence changes. For example, in the highly turbulent system being illustrated here, much of the mean-flow kinetic energy feeds into large-scale turbulence, whereas thermal energy receives much of its energy from small-scale turbulence.



Even for a single fluid with constant, uniform density the relevant mathematical formulations are lengthy, and there are significant difficulties yet to be resolved. Nevertheless, we can capture in a relatively; simple manner much of the flavor of turbulence modeling by starting with the Navier-Stokes fluid-dynamics equations for an incompressible fluid—that is, a fluid of constant density and viscosity everywhere and for all time. One of our fundamental assumptions is that these familiar and deceptively simple equations describe everything we need to understand about the turbulence of such a fluid, including every “microscopic” detail in every fluctuating part of the turbulent flow.

The Navier-Stokes equations describe the variations of pressure and velocity in the fluid. Using Cartesian index notation with The summation convention, we can write the first equation, which is an expression of The conservation of mass, as

$$\frac{\partial u_i}{\partial x_i} = 0. \tag{9}$$

and the second, which is an expression of the conservation of momentum, as

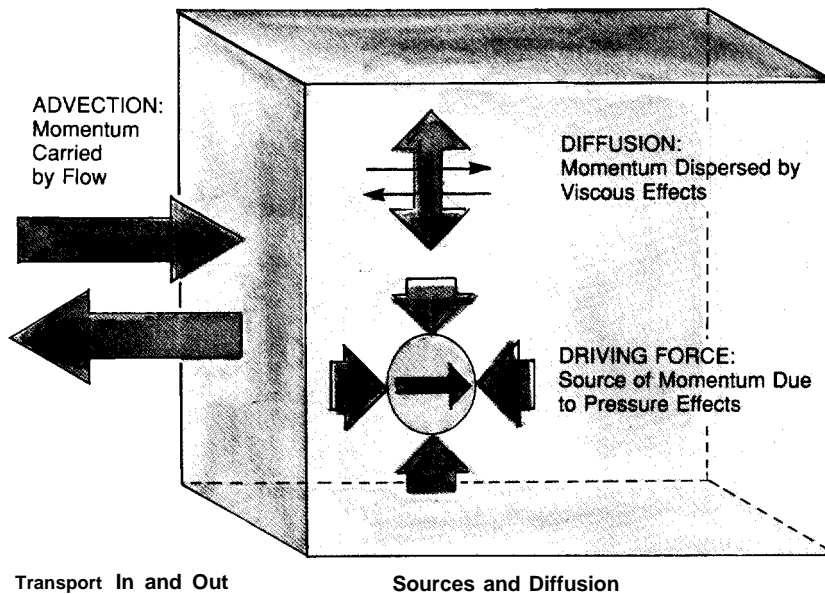
$$\frac{\partial u_i}{\partial t} + \frac{\partial u_i u_j}{\partial x_j} = -\frac{\partial p}{\partial x_i} + \nu_m \frac{\partial^2 u_i}{\partial x_k^2} \tag{10}$$

Rate of
Advection
Driving
Diffusion
Change

Force

MOMENTUM TRANSPORT

Fig. 10. The diffusion, driving-force, and advection terms of the Navier-Stokes momentum equation represent the ways in which momentum is locally added to or taken away from a region in the fluid.



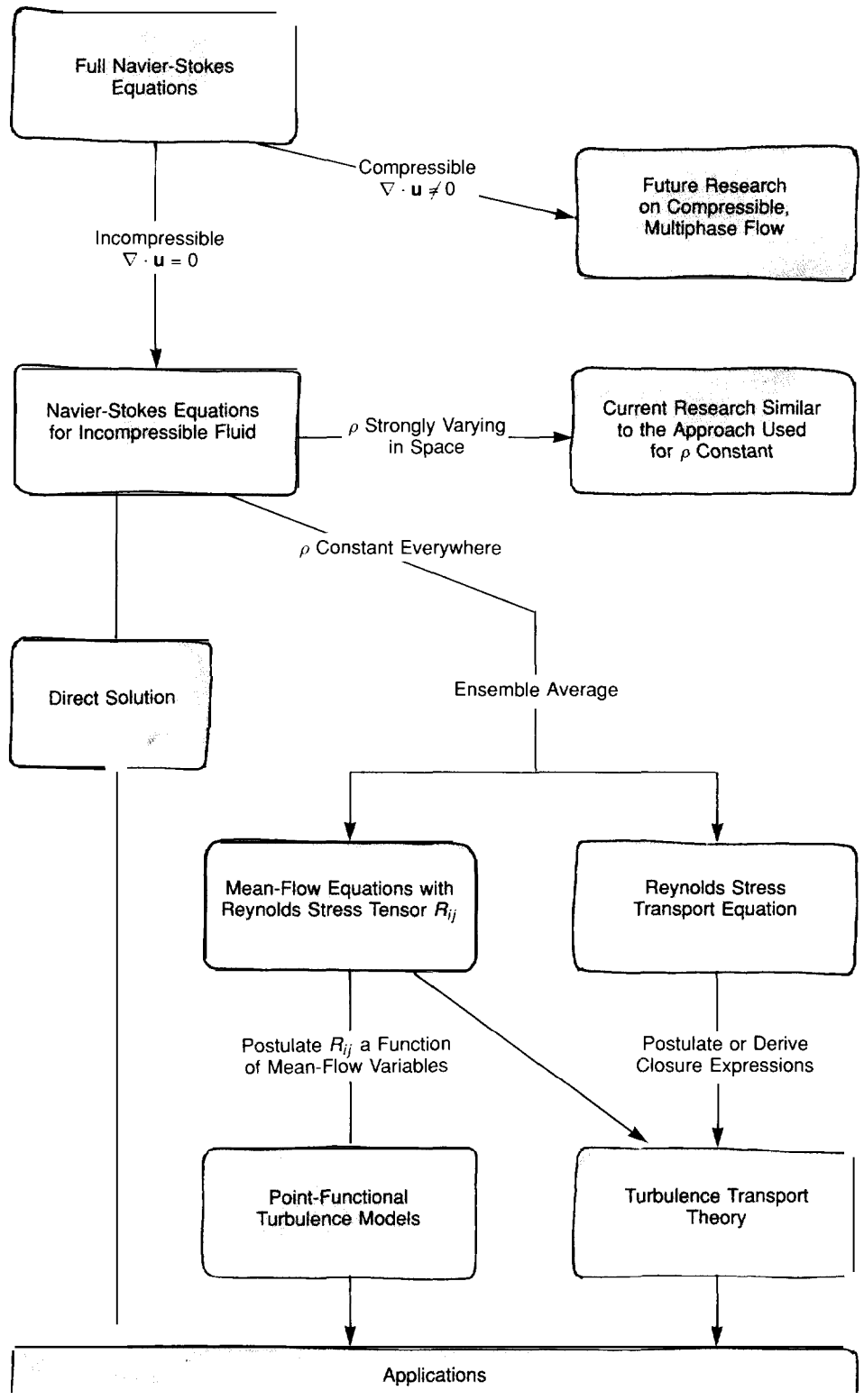
Here ν_m is the molecular *kinematic* viscosity coefficient (the ratio of molecular viscosity to density μ_m/ρ), u_i is the i th component of the vector velocity, and p is the ratio of pressure to density. Figure 10 illustrates the effects of the various terms in the momentum equation.

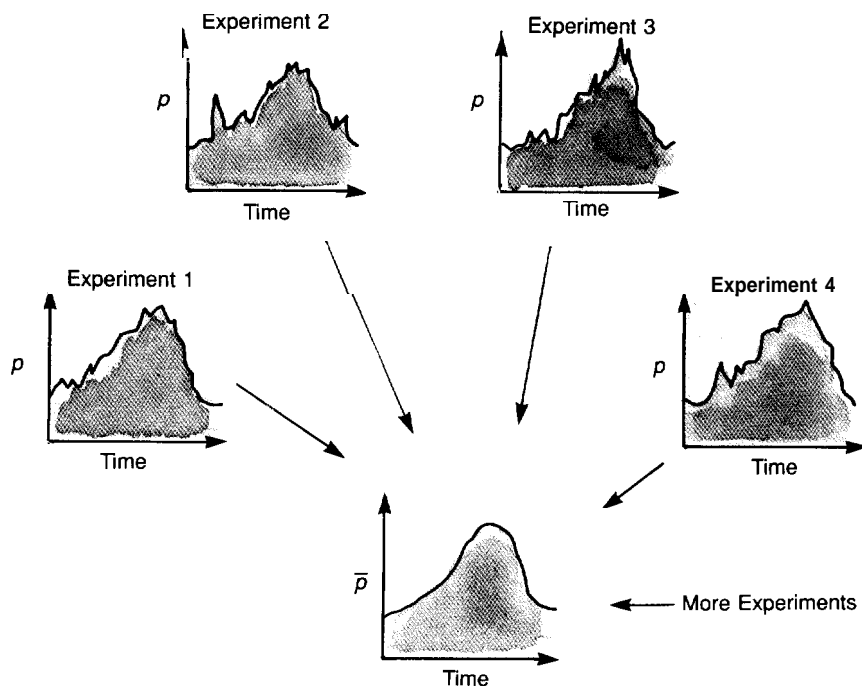
So, there it is in a nutshell: the entire, mysterious world of turbulent fluid flow described by two short lines of mathematical symbols. Well, not quite the entire *real* world, because many fluids are not the idealized incompressible materials of constant viscosity and density considered here, but we shall return to that point below.

One obvious approach to modeling turbulence is to solve the Navier-Stokes equations directly (the left path in Fig. 11). However, certain difficulties limit the success of this approach. For example, even when the mean flow is one-dimensional, the equations must be solved numerically in three dimensions because turbulence is inherently three-dimensional. Only recently have computers had enough computational capability to begin meeting the task of solving three-dimensional fluid-flow problems. To describe the full spectrum of eddies, the computational mesh would have to be fine enough for the smallest eddies, yet cover a domain large enough to include the mean flow and the largest eddies. Another complication occurs if the system includes a solid boundary. Because the turbulent flow depends on the minute details of the boundary conditions (even *stochastic* quantities depend on minute perturbations in the initial and boundary conditions, such as wall roughness), these details must be specified. Furthermore, because a particular set of minute perturbations describe only one possible representation of the boundary conditions, repeated calculations must be made with various boundary conditions and the results of the calculations averaged to give a complete description of the turbulent flow. The memory and speed requirements for the calculations would

**APPROACHES TO
TURBULENCE MODELING**

Fig. 11. Typically, modeling of turbulence makes two simplifying assumptions with respect to the full Navier-Stokes equations: an incompressible fluid ($\nabla \cdot \mathbf{u} = 0$) and the density ρ constant everywhere. Using just the first of these assumptions, one could, in principle, solve the equations directly (left path)—a difficult task. However, if one uses *both* simplifying assumptions together with ensemble averaging, the result is two sets of equations: the mean-flow equations, which include the Reynolds stress tensor R_{ij} , and the Reynolds stress transport equation. Turbulence transport theory (right) uses input from both sets, whereas point-functional turbulence models (middle) deal only with the mean-flow equations (by postulating that R_{ij} is a function of mean-flow variables). Later in this article we describe work on multiphase flow in which the assumption of constant density has been dropped. Current research is just beginning to approach the full Navier-Stokes equations for compressible, multiphase flow.





ENSEMBLE AVERAGING

Fig. 12. Consider a series of experiments, each conducted with the same initial and boundary conditions. For each, we determine the pressure p at a particular point in space as a function of time. An average of all these experiments would represent an ensemble average.

tax even the most powerful of our modem computers. If these calculations could be accomplished, however, the *advantage* of a direct calculation of turbulence would be that no approximations or empirical postulates are required.

Ensemble Averages. Largely for the reasons given above, almost all theoretical approaches to turbulence modeling use some type of averaging--either temporal, spatial, or ensemble. With the proper statistical treatment, the solution of turbulent flow problems need not resolve the full spectrum of eddies, initial and boundary conditions need not be specified in minute detail, and a flow whose mean velocity is one-dimensional can be numerically calculated in one dimension even though the resolved turbulence is three-dimensional. However, with these advantages for turbulence transport modeling come the disadvantages of assumptions and approximations needed to obtain a set of solvable equations.

What is meant by the average of any flow variable in a turbulent flow? Time averages are easy to understand. We say that fluid flow is statistically steady if the time average of many fluctuations at some point in space is independent of the averaging period chosen. Spatial averages, likewise, are easy to visualize but are relevant only when the structural scale of the turbulence is very small compared with that of the mean-flow fluctuations--a relatively rare condition. Here we will focus on ensemble averaging, which is the most general type of averaging with the fewest restrictions.

We can intuitively sense what an ensemble average is if we imagine a very large number of experiments, all with the same macroscopic initial and boundary conditions, but each with its own particular realization of the turbulent part of the flow (Fig 12). The ensemble average of some flow parameter at any given point and time is then the

average of that parameter over all the experiments. For the condition of steady flow, time and ensemble averages are the same.

The ensemble average is most conveniently formulated in terms of *moments* of an appropriate distribution function. (Here, rather than integral nomenclature, we will simply use an overline to designate an ensemble average.) Thus \bar{p} is the moment, or ensemble average, of the pressure (per unit density), and $\overline{p u_i}$ is the ensemble average of the product of pressure and the i th component of fluid velocity. (Note that $\overline{p u_i}$ does not necessarily equal $\bar{p} \bar{u}_i$.)

For each experiment in a series, detailed measurements give p and u_i , both of which fluctuate strongly as a function of position and time. Likewise, \bar{p} and \bar{u}_i vary with position and time but in a much calmer fashion. The difference between the individual experimental value and the ensemble average is the fluctuating part of the variable, denoted by a prime: $p' \equiv p - \bar{p}$; $u_i' \equiv u_i - \bar{u}_i$. The ensemble average of this fluctuating part must be zero for each variable (that is, $\overline{p'} = 0$ and $\overline{u_i'} = 0$), but it does not follow that the moment, or ensemble average, of a product of fluctuational variables (such as $\overline{p' u_i'}$ or $\overline{u_i' u_j'}$) vanishes. Indeed, the essence of our turbulence modeling is contained in the behavior of such ensemble averages of fluctuational products.

Reynolds-Stress Transport Equation. One of these fluctuational products, the Reynolds stress tensor, is especially important; it is defined by

$$R_{ij} \equiv \overline{u_i' u_j'}. \quad (11)$$

Notice that the contraction of the Reynolds stress tensor (that is, when $i = j$) is exactly twice the turbulence kinetic energy per unit mass of fluid ($R_{ii} \equiv \overline{u_i' u_i'} = 2K$).

The importance of R_{ij} in turbulence modeling can be demonstrated quite handily. First we rewrite the Navier-Stokes equations, expressing each of the variables as the sum of its mean and fluctuating parts:

$$\frac{\partial (\bar{u}_i + u_i')}{\partial x_i} = 0$$

and

$$\frac{\partial (\bar{u}_i + u_i')}{\partial t} + \frac{\partial}{\partial x_j} [(\bar{u}_i + u_i') (\bar{u}_j + u_j')] = -\frac{\partial (\bar{p} + p')}{\partial x_i} + \nu_m \frac{\partial^2 (\bar{u}_i + u_i')}{\partial x_k^2}. \quad (12)$$

Then we take the ensemble average of these equations (commuting averages and derivatives where necessary and remembering that the average of a single fluctuating variable is zero) and obtain the *mean-flow equations*:

$$\frac{\partial \bar{u}_i}{\partial x_i} = 0$$

and

$$\frac{\partial \bar{u}_i}{\partial t} + \frac{\partial}{\partial x_j} (\bar{u}_i \bar{u}_j) = -\frac{\partial \bar{p}}{\partial x_i} - \frac{\partial R_{ij}}{\partial x_j} + \nu_m \frac{\partial^2 \bar{u}_i}{\partial x_k^2}. \quad (13)$$

A single term involving the Reynolds stress has emerged, and we see that the *only* effect of turbulence on the mean flow is through the addition of that term to the equations. We note in passing that Eqs. 13 form the basis of *point-functional turbulence models* (the middle branch in Fig. 11) and will return to this point shortly.

The mean-flow equations (Eqs. 13) can be subtracted from the full equations (Eqs. 12) to show that the fluctuating parts of the variables obey the equations

$$\frac{\partial u'_i}{\partial x_i} = 0 \quad (14a)$$

and

$$\frac{\partial u'_i}{\partial t} + \frac{\partial}{\partial x_j} \left(\overline{u_i u'_j} + u'_i \overline{u_j} + u'_i u'_j - \overline{u'_i u'_j} \right) = -\frac{\partial p'}{\partial x_i} + \nu_m \frac{\partial^2 u'_i}{\partial x_k^2}. \quad (14b)$$

We need Eqs. 14 to derive the *Reynolds-stress transport equation*, that is, a description of the behavior of the Reynolds stress itself (the right branch of Fig. 11). This derivation is straightforward but tedious. We merely note that the following steps are involved:

1. multiply Eq. 14b by u'_j to obtain Eq. 14c,
2. interchange i and j in Eq. 14c to obtain Eq. 14d,
3. add Eqs. 14c and 14d, and
4. take the ensemble average.

With some rearrangement of terms and the identification of R_{ij} in several places, the result is

$$\begin{aligned} \frac{\partial R_{ij}}{\partial t} &+ \frac{\partial \overline{u_k} R_{ij}}{\partial x_k} + R_{ik} \frac{\partial \overline{u_j}}{\partial x_k} + R_{jk} \frac{\partial \overline{u_i}}{\partial x_k} + \frac{\partial \overline{u'_i u'_j u'_k}}{\partial x_k} = \\ \text{Rate of} & \quad \text{Advection} \quad \text{Mean-Flow Source} \quad \text{Triple} \\ \text{Change} & \quad \quad \quad \text{and Rotation} \quad \text{Correlation} \\ & - \overline{u'_i \frac{\partial p'}{\partial x_j}} - \overline{u'_j \frac{\partial p'}{\partial x_i}} + \nu_m \left(\frac{\partial^2 R_{ij}}{\partial x_k^2} - 4D_{ij} \right), \quad (15) \\ & \quad \quad \text{Driving Force} \quad \quad \quad \text{Diffusion} \quad \text{Decay} \end{aligned}$$

in which

$$D_{ij} = \frac{1}{2} \frac{\partial \overline{u'_i u'_j}}{\partial x_k} \frac{\partial \overline{u'_i u'_j}}{\partial x_k}. \quad (16)$$

We now can distinguish the turbulence-transport theories and their predecessors, the point-functional turbulence theories. As we remarked earlier, point-functional turbulence theories use Eqs. 13 by postulating a form for the Reynolds stress R_{ij} that is a function of the mean-flow variables themselves. As a result, such theories are called “point-functional” because the description of the turbulence at some point in the flow depends only on the current value of the mean-flow variables. Point-functional theories have the advantage of being as easy to solve as the original Navier-Stokes equations but have the shortcoming that the theories are largely empirical and have limited regions of applicability.

TURBULENCE TRANSPORT

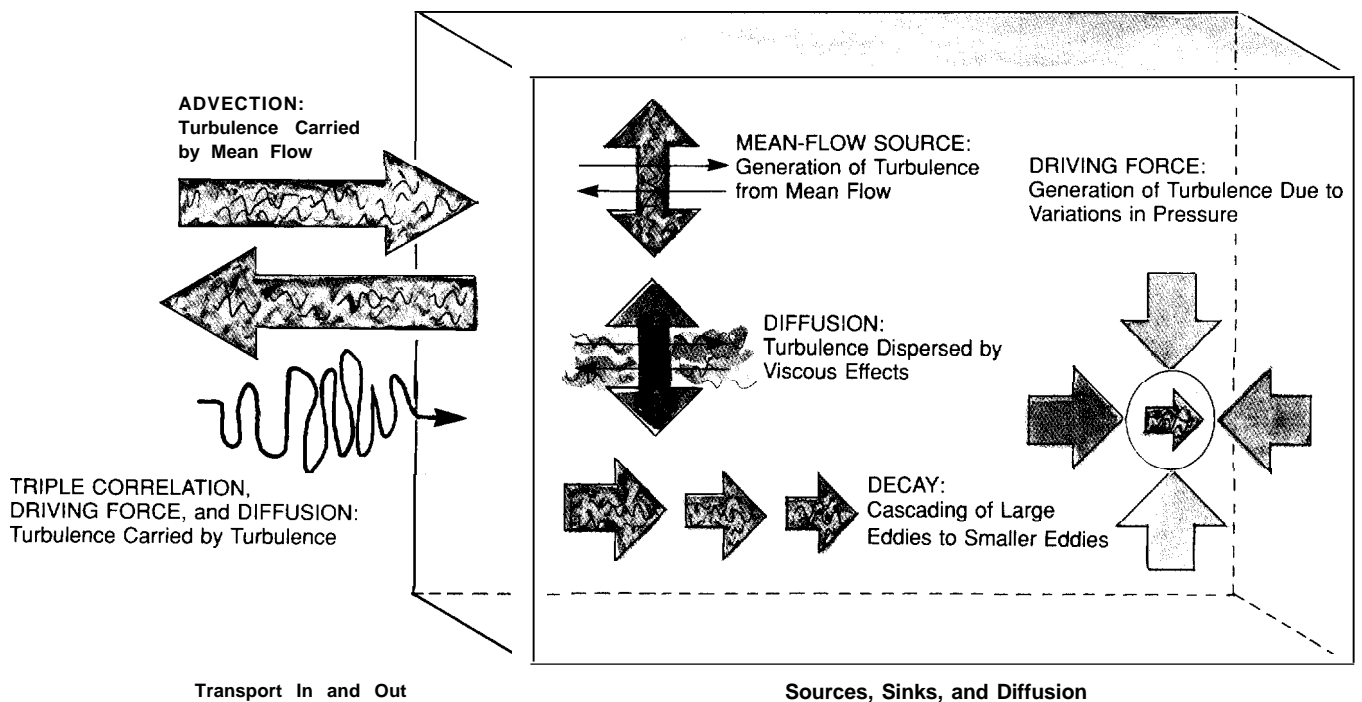
Fig. 13. Just as Fig. 10 illustrates the various terms of the Navier-Stokes momentum equation, this figure illustrates the various terms of the Reynolds-stress transport equation. The driving force and the diffusion terms appear twice because each can be decomposed into a contribution to the transport of turbulence and a contribution to the generation or diffusion of turbulence.

In contrast to point-functional theories are the *history-dependent*, or *turbulence-transport*, theories. These theories, the focus of our interest here, include a set of one or more *auxiliary* equations that describe the history, or transport, of the variables associated with turbulence and that are solved in conjunction with the mean-flow equations (Eqs. 13). The auxiliary equations can range from empirical postulations to some form of the Reynolds transport equation (Eq. 15).

Because our starting point was the Navier-Stokes equations, turbulence-transport theory based on Eqs. 13 and 15 should, in principle, contain all the necessary information to describe the mean properties of turbulent flow. However, in practice it is necessary to introduce additional constraints or empirical information to yield a solvable set of equations. This procedure of “closing” the set of governing equations is called *closure modeling* and plays a central role in turbulence-transport theory.

The development of a solvable set of equations is beyond the scope of this article (although, in the following section we do so for a simple treatment of turbulence). We can nevertheless capture much of the flavor of the necessary developments by considering the significance of the terms in the Reynolds transport equation (Fig. 13 graphically illustrates the nature of each) and by considering the difficulties of describing their properties in terms of the macroscopically accessible mean-field quantities.

Advection, Mean-Flow Source, and Rotation. The advection and the mean-flow source and rotation terms of Eq. 15 contain only the unknown tensor R_{ij} and the mean-flow velocities; no reference to the detailed turbulence structure occurs. These terms constitute a bulwark of settled mathematical structure for which there are essentially no uncertainties or controversies about the physics. In essence they describe the manner



in which the mean flow moves turbulence from one place to another by translation, rotation, and stretching or contraction of the fluid.

Triple Correlation. The triple-correlation tensor $\overline{u'_i u'_j u'_k}$ that appears in the next term in Eq. 15 is usually interpreted as a diffusive flux of the Reynolds stress generated by the action of the stress itself. Thus, this term can be called the turbulence self-diffusion term because it describes the turbulent diffusion of turbulence.

We can show in more detail how this identification is made and, at the same time, illustrate what is meant by closure modeling. If Q represents some quantity (such as the concentration of a dissolved, neutrally-buoyant substance) that is purely advected by the incompressible fluid, its transport equation is simply

$$\frac{\partial Q}{\partial t} + \frac{\partial(Qu_i)}{\partial x_i} = 0. \quad (17)$$

Decomposing the variables into mean and fluctuating parts and taking the ensemble average (as we did before with Eqs. 12 and 13), we find that

$$\frac{\partial \overline{Q}}{\partial t} + \frac{\partial(\overline{Q}u_i)}{\partial x_i} = -\frac{\partial \overline{Q'u'_i}}{\partial x_i}. \quad (18)$$

Since the right side describes the diffusion of Q due to the effects of turbulence, we directly identify $\overline{Q'u'_i}$ as a diffusive flux. Just as the flux of a chemical species is proportional to its concentration gradient (Fick's law), the diffusive flux is proportional to the gradient of Q itself:

$$\overline{Q'u'_i} \propto \frac{\partial \overline{Q}}{\partial x_i}. \quad (19)$$

The proportionality constant is a function of the turbulence intensity; indeed, more detailed considerations indicate that

$$\overline{Q'u'_i} \approx -\left(\frac{s}{\sqrt{2K}}\right) R_{il} \frac{\partial \overline{Q}}{\partial x_l}, \quad (20)$$

in which s is the length scale of the turbulence. It follows that

$$\overline{u'_i u'_j u'_k} \equiv \overline{R'_{ij} u'_k} \approx -\left[\frac{s}{(2K)^{1/2}}\right] R_{klt} \frac{\partial R_{ij}}{\partial x_l} \quad (21)$$

In this manner, we see what is meant by closure modeling, that is, the elimination of any residual reference to details of the turbulence. For our purposes we need not delve any deeper into this aspect of turbulence modeling; the example is sufficient to indicate some of the heuristic and empirical procedures we inevitably have been forced to employ.

Driving Force. The pressure-velocity correlation terms (the first two terms on the right side of Eq. 15) are especially important to the transport modeling of turbulence. They describe one of the principal driving forces by which mean-flow energy finds its way

into fluctuations. Moreover, they contribute significantly to the isotropic rearrangement of anisotropic turbulence.

The unstable slip plane of Fig. 6a is excellent for visualizing the effects of these terms. Previously, we observed that on either side of the slip plane a slight increase in velocity over the mean for that side is accompanied by a slight decrease in the pressure, whereas exactly the opposite occurs in the other half of the fluid. Thus, fluctuations in pressure and velocity are strongly correlated. Because u'_x and $\partial p'/\partial y$ have opposite signs (for example, an increase in u'_x in the lower half results in a downward or negative pressure gradient), the ensemble average of the product of these variables is always negative. But the two $\overline{u'_i \frac{\partial p'}{\partial x_i}}$ terms in Eq. 15 are negative, so these terms are a *positive* source to R_{xy} (that is, to the *anisotropic, or off-diagonal, components* of the Reynolds stress tensor).

Once R_{xy} is created, it ultimately contributes to the turbulence kinetic energy K , which, as we noted earlier, is proportional to R_{ii} (that is, to the sum of *diagonal components* of the stress tensor). That R_{xy} contributes to K is easily illustrated by examining the contracted form of the Reynolds stress transport equation for, say, the type of flow illustrated in Fig. 5. In this case, the mean-flow source terms contribute to the rate of change only as follows:

$$\frac{\partial R_{ii}}{\partial t} \equiv 2 \frac{\partial K}{\partial t} = -2R_{xy} \frac{\partial \bar{u}_x}{\partial y}. \quad (22)$$

Hence, the anisotropic, or off-diagonal, components of R_{ij} , once created by the mean flow from the driving-force terms, eventually contribute to the turbulence kinetic energy through the mean-flow source terms.

Diffusion and Decay. Of the last two terms in Eq. 15, the first is usually negligible and represents diffusion of turbulence by molecular viscosity, which requires no further modeling. The second involves the tensor D_{ij} , for which the usual procedure has been to derive a horrendously complicated transport equation and attempt to solve this simultaneously with the Reynolds transport equation. Such a procedure introduces a host of additional correlation terms to be modeled, and much appeal to “intuition” is invoked in the process.

Bypassing the fascinating but tedious discussion of these derivations, we can nevertheless describe several interesting properties of this second term. First, its contraction

$$D_{ii} \equiv \frac{1}{2} \overline{\left(\frac{\partial u'_i}{\partial x_k} \right)^2} \quad (23)$$

is positive definite so that the $-4\nu_m D_{ij}$ term in Eq. 16 always describes a *decay* of the turbulence energy.

The second interesting property, deduced by extensive manipulations of the D_{ij} transport equation, is that D_{ij} should vary inversely as the molecular viscosity under almost all circumstances. Therefore $\nu_m D_{ij}$ is essentially independent of viscosity, which seems paradoxical. Resolution of this paradox hinges on an important property of turbulence: most of the turbulence effects and energy are associated with the largest of

the eddies, which decay first by cascading to smaller eddies before converting to thermal energy (Fig. 9). Thus, an alternative to the usual modeling of the behavior of D_{ij} has recently emerged. We can get the same results by treating the decay of the large-scale eddies as the energy source of the small-scale eddies. For this purpose the large-scale eddies are momentarily thought of as being “mean flow.” In some complicating circumstances, such as interpenetration of particles, this alternative modeling technique has proven so far to be the only tractable approach.

Simpler Transport Models and Examples of Their Application

Some problems do not warrant the degree of complexity and closure approximation required to numerically solve the full Reynolds-stress transport equation. A more conventional and practical approach uses the following approximation (called Boussinesq’s approximation) for turbulence stresses in an incompressible **fluid**:

$$R_{ij} = -\nu_t \left(\frac{\partial \bar{u}_i}{\partial x_j} + \frac{\partial \bar{u}_j}{\partial x_i} \right) + \frac{2}{3} K \delta_{ij}, \quad (24)$$

in which ν_t , the *turbulence* viscosity, is a measure of the increase in viscosity due to turbulence (see “Reynolds Number” and “Reynolds Number Revisited”), and δ_{ij} is the Kronecker delta function ($\delta_{ij} = 0$ if $i \neq j$, $\delta_{ij} = 1$ if $i = j$, and $\delta_{ii} = 3$). This approximation is consistent with the definition of turbulence kinetic energy in terms of the Reynolds stress: $R_{ii} = 2K$. Furthermore, the approximation bears a strong resemblance to the Stokes formulation for laminar-flow stresses p_{ij} , in which the stresses are related to *molecular* viscosity and fluid pressure (rather than turbulence viscosity and kinetic energy):

$$p_{ij} = \nu_m \left(\frac{\partial \bar{u}_i}{\partial x_j} + \frac{\partial \bar{u}_j}{\partial x_i} \right) - p \delta_{ij}. \quad (25)$$

The chief advantage of using Boussinesq’s approximation is that transport relationships for all individual components of R_{ij} are replaced by a single expression involving an effective turbulence, or eddy, viscosity.

How does one describe ν_t ? The simplest imaginable description of the turbulence viscosity is that it is a constant that depends on some average mean-flow parameters. Somewhat better is a formulation that relies on a mixing length l , which is usually an algebraic estimate of the size of the main energy-containing eddies as a function of flow geometry. For example, one approach that has proven quite successful for boundary-layer flow and some other well-defined jet flows is to define ν_t by modifying Prandtl’s mixing-length theory so that

$$\nu_t = l^2 \frac{\partial \bar{u}}{\partial n}. \quad (26)$$

In this equation, n is the local distance to a rigid object or axis of symmetry and u is a representative free-stream velocity. Note that Eq. 26 makes ν_t a function of mean-flow parameters only and is thus an example of point-functional modeling.

Reynolds Number Revisited

As discussed in the earlier sidebar, the Reynolds number is a convenient and physically sound basis for comparing similar flows under different circumstances. For instance, as flow speed through a pipe increases, the drag on the fluid increases and, consequently, so also does the required applied pressure; these increases are reflected in a corresponding increase in Reynolds number. Total friction experienced by the fluid undergoing laminar flow is usually expressed in terms of the Reynolds number R , allowing easy comparison between widely varying tests.

Once the Reynolds number reaches a critical value, however, laminar flow in the pipe becomes turbulent, and further increases in Reynolds number no longer reflect significant changes in measured drag. At this point, the effective turbulence Reynolds number R_{eff} becomes a more appropriate gauge, reflecting the ratio of inertial to turbulence momentum-dissipation effects (rather than inertial to viscous-dissipation effects).

Although the Reynolds number can, in theory, be increased without bound, the turbulence Reynolds number cannot. The value of R_{eff} is not directly and uniquely set by readily measured properties and flow geometry but rather depends on eddy generation and the resulting eddy sizes within the flow field. A limiting value of R_{eff} is observed in turbulent-flow experiments.

To demonstrate this behavior quantita-

tively, it is convenient to make some simplifying assumptions. Typically, the turbulence viscosity ν_t , which is much larger than the molecular viscosity ν_m , is taken to be equal to the product of eddy size s (the turbulence length scale), an appropriate turbulence velocity (here taken as $K^{1/2}$, where K is the specific turbulence kinetic energy), and a universal constant $1/C_\nu$. Thus

$$R_{\text{eff}} \approx C_\nu \frac{u_0 L}{s K^{1/2}}, \quad (1)$$

where L is a characteristic length for the mean flow.

If, as is usually the case, the turbulence kinetic energy is some fraction of the mean-flow kinetic energy ($K \cong \frac{1}{2} f_K u_0^2$), then

$$R_{\text{eff}} \cong C_\nu \sqrt{\frac{2}{f_K}} \left(\frac{L}{s} \right); \quad (2)$$

that is, R_{eff} is proportional to the ratio of the length scales. As turbulence gains in intensity, its *average* length scale usually decreases slightly, but not without limit. In fact, the largest eddies, those that contain the major fraction of the turbulence kinetic energy, will be some portion of the mean-flow length scale (such as pipe diameter). Therefore, since C_ν is usually about 10 and an upper bound on L/s is typically 20, R_{eff} will seldom exceed several hundred, even in the most intensely turbulent flows. On the other hand, R can be several million or more. ■

For more complex flows the simplifications introduced through Eq. 26 are not justified, and a transport model that details evolution of ν_t , or quantities related to it, is needed. Although this approach is viable only at the expense of much added complexity, it has recently been favored by investigators working with the complicated flow patterns of high-speed jets, shock-boundary-layer interactions, and two-phase flows.

To produce a simplified transport description of turbulence, we rely on flow properties already introduced to develop a dimensionally correct form of ν_t . For example,

$$\nu_t \equiv \frac{C_\nu K^2}{2\nu_m D_{ii}} = C_\nu \frac{K^2}{\epsilon}, \quad (27)$$

where C_ν is a model constant, hopefully universal in its applicability, and $\epsilon = 2\nu_m D_{ii}$. The last parameter, ϵ , is related to the mean rate of dissipation of turbulence kinetic energy and, as discussed in the earlier section entitled "Diffusion and Decay," is independent of molecular viscosity.

From this definition of turbulence viscosity, we can generate transport equations for ϵ and K . For instance, after performing the tensor contraction of the Reynolds transport equation (Eq. 15) and introducing appropriate closure expressions, we obtain the following simplified transport equation for K :

$$\frac{\partial K}{\partial t} + \overline{u_k} \frac{\partial K}{\partial x_k} = \frac{\partial}{\partial x_k} \left(\frac{\nu_t}{\sigma_K} \frac{\partial K}{\partial x_k} \right) + \nu_t \left(\frac{\partial \overline{u_i}}{\partial x_k} + \frac{\partial \overline{u_k}}{\partial x_i} \right) \frac{\partial \overline{u_i}}{\partial x_k} - \epsilon. \quad (28)$$

Here σ_K is a model constant of order one, and, because of Eq. 27, ν_t is itself a function of K and ϵ .

Next, a treatment similar to that used earlier to split the flow variables into mean and fluctuating parts is applied to the Navier-Stokes momentum equation to create a transport equation for D_{ij} . Again, after contraction and closure modeling, we get the following transport equation for ϵ :

$$\frac{\partial \epsilon}{\partial t} + \overline{u_k} \frac{\partial \epsilon}{\partial x_k} = \frac{\partial}{\partial x_k} \left(\frac{\nu_t}{\sigma_\epsilon} \frac{\partial \epsilon}{\partial x_k} \right) + \frac{C_1 \epsilon \nu_t}{K} \left(\frac{\partial \overline{u_i}}{\partial x_k} + \frac{\partial \overline{u_k}}{\partial x_i} \right) \frac{\partial \overline{u_i}}{\partial x_k} - \frac{C_2 \epsilon^2}{K}, \quad (29)$$

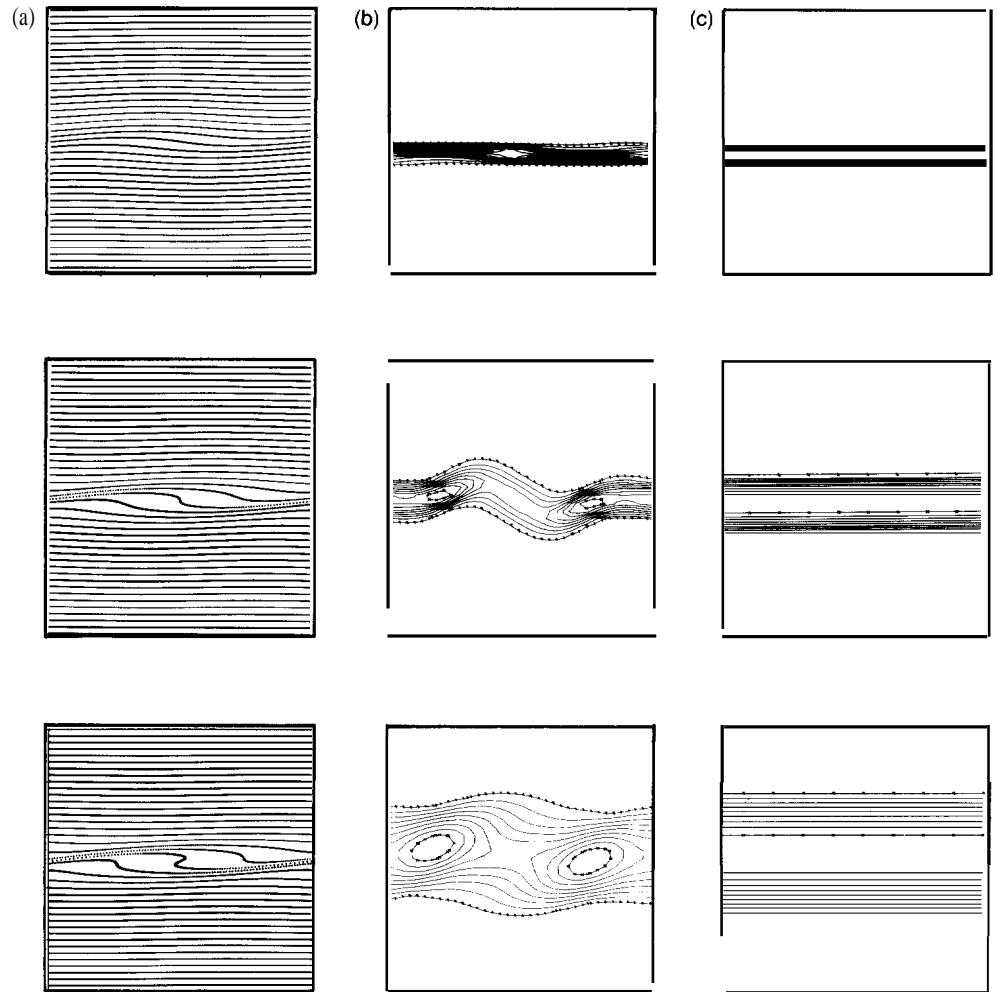
where C_1 , C_2 , and σ_ϵ are model constants, all of order one.

To show how we apply this model, we return to the problem of turbulence in a slip plane (Fig. 6). Our goal is to demonstrate numerically that turbulence is indeed generated by such a configuration and that we can follow its development throughout a two-dimensional flow field as a function of time and position. We use three different methods of accounting for the turbulence and discuss the pros and cons of each.

The first method involves direct solution of the Navier-Stokes equations by a finite-difference method as an approximation to the left path in Fig. 11. Our calculations use a two-dimensional velocity field, and turbulence below the scale of the computational grid is thus ignored. We assume that a slight, sinusoidal vertical velocity is imparted to the interface separating the oppositely flowing fluids. The maximum speed of this perturbation is only 1 per cent of the mean translational speed (and thus the kinetic energy associated with the perturbation is, at most, 10^{-4} times the mean-flow kinetic energy).

THREE SIMPLIFIED TURBULENCE CALCULATIONS

Fig. 14. The evolution in time (from top to bottom) of the turbulence in the slip-plane problem of Fig. 6, as determined by three different types of simplified calculations. In (a), a large-scale sinusoidal perturbation in the vertical direction is calculated with full equations without modeling the unresolved turbulence. The marker-particle plot (corresponding to mean-flow streaklines) in the third panel shows that a slip-plane instability is a strong source of perturbation in the velocity field. In (b), the perturbational energy of (a) has been increased 10 per cent with the addition of small-scale fluctuations. These fluctuations are accounted for with a turbulence kinetic energy K and its transport equation, and the panels show contour plots of K . This more realistic approach reveals a faster growth in the turbulence. Finally, in (c), all the perturbational energy (both small- and large-scale motion in the vertical direction) is accounted for as turbulence kinetic energy. From this perspective, mean flow can only be horizontal and thus varies in only one (vertical) direction. The contour plots of turbulence kinetic energy show the same growth rate as in (b) for mixing between the layers of undisturbed flow.



The results of our calculations are shown in the left column of Fig. 14 as *marker-particle plots* in which the lines correspond to mean-flow streaklines (representing what you would see if you had introduced a stream of smoke). As time progresses (from top to bottom in the figure), we see that the width of the mixing layer spreads and displays wave-like structures characteristic of the Kelvin-Helmholtz instability. Thus, our calculations show that a slip-layer instability is indeed a strong source of turbulent mixing.

A more interesting and realistic approach incorporates simplified transport of turbulence in the calculations. Consider the same flow, only with additional small-scale sinusoidal perturbations superimposed on the initial large-scale perturbation. If we were to use the first method and treat these minute fluctuations as part of the resolved flow, we would need a much finer computational grid to resolve the details of the velocity field. Rather than do this, we account for the microscopic perturbations through a turbulence kinetic energy K and its corresponding transport equation, then plot the results of our calculations as contour plots of K . This model is more realistic because the kinetic-energy variable incorporates all length scales of turbulence, as well

as the three-dimensionality.

For our simplified transport calculation, we assume the same large-scale perturbation (with an energy 10^{-4} times the mean-flow kinetic energy) and then add a further 10 per cent (or 10^{-5} times the mean-flow energy) in small-scale energy. Our results (the second column of Fig. 14) show that accounting for small-scale perturbational energy causes the growth rate of the turbulence to be much larger than in the first method.

We should also note that even though turbulence is inherently three-dimensional, both the first and second methods deal with *mean flow* in two dimensions. In the second case, however, we are able to account for the third dimension in an average sense via turbulence kinetic energy and its transport.

A third approach is to treat *all* length scales as turbulence—even the large-scale perturbation, which, so far, has been treated as part of the mean flow. We can do this because the exact definition of turbulence is a relative one that depends on the observer's point of view. If we adopt this scheme, the flow becomes *one-dimensional*, that is, only vertical *changes* occur in \bar{u} , K , and ϵ .

In our calculations with this method, we assume the same *total* initial perturbational energy as in the second example, but with the large- and small-scale energies lumped together. Once again, all length scales of turbulence are incorporated, and our results (the third column of Fig. 14) show that the growth rate of the layer matches that in the second example very closely. On the other hand, turbulence on the largest length scale, which corresponds to mean flow in the earlier examples, is not resolved in detail.

Thus, to effectively use turbulence modeling, one must decide which length scales will be considered mean flow and which will be considered turbulence. Once this has been decided, the power of the method allows us to describe the flow accurately without having to dedicate excessive computer resources to resolving minute flow structures in detail.

Current Research

So far we have concentrated on turbulence in a single incompressible fluid with density perfectly constant in position and time (the downward branches of Fig. 11). Recently, our research has included additional features that are of interest to many of the new scientific and engineering directions at Los Alamos and other laboratories. These features are

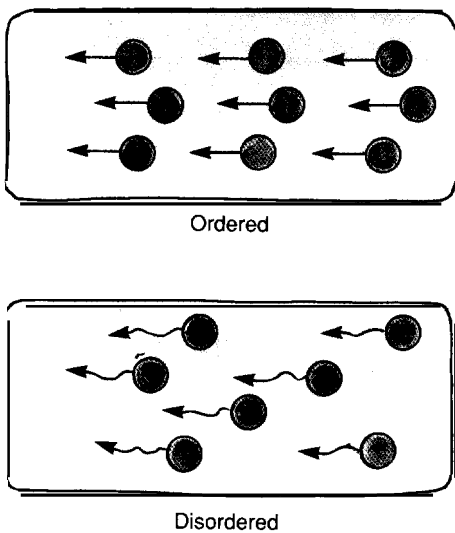
- . Two-phase flow interactions: the sources, sinks, and effects of turbulence in a fluid containing particles, droplets, or bubbles of another material.
- Density gradients: turbulence in an incompressible fluid for which variations of temperature or the presence of some dissolved substance cause large variations in density.
- Supersonic turbulence: the effects of high-speed processes on turbulence.

In all cases, we continue to use the basic philosophy of transport modeling, which, despite some obvious difficulties, seems at present to be by far the most promising approach for the solution of practical problems.

Two-Phase Flow. Particles, drops, or bubbles suspended in a fluid—whether that fluid is a liquid or a gas—can significantly alter the turbulence and its effects. Intuitively,

TWO-PHASE INTERPENETRATION

Fig. 15. Our transport modeling techniques are able to handle both ordered interpenetration of two phases, such as occurs in the laminar-flow transport of blood cells, and disordered interpenetration, such as occurs in a rapidly moving gas that contains suspended particles.



we expect that when distinct entities interpenetrate a surrounding fluid the *creation* of turbulence is enhanced; on the other hand, we also expect the inertial properties of heavy entities to dampen turbulent fluctuations. How can we describe these effects quantitatively?

From considerations similar to those for incompressible flow of a single fluid, we know that extra turbulence is generated by pressure gradients producing *differences* in the accelerations of the particles and of the surrounding fluid. Such differential acceleration induces distortions of the fluid around the particles, thereby creating disturbances in the velocity field that would be absent if there were no particles.

For example, consider the flow field of a shock wave moving horizontally and passing a rigid particle suspended in the fluid. If no particle was present, the flow would remain completely horizontal. However, as the shock wave passes the particle, local velocity fluctuations appear, including changes in the horizontal velocity and the generation of vertical velocity. As soon as there is a velocity difference between the velocity fields of the particle and the fluid, viscous drag forces, competing with differential acceleration, begin to diminish any velocity perturbations.

In a manner analogous to that for single-phase flow, the relative contributions of acceleration and viscous drag can be compared through a *particle* Reynolds number

$$R_p = D_p \frac{|\overline{u_f} - \overline{u_p}|}{\nu_m}, \quad (30)$$

where D_p is the particle diameter, u_p and u_f are the local velocities of the particle and fluid, respectively, and ν_m is the molecular kinematic viscosity of the fluid.

Consider a shock moving with a high velocity through a collection of particles that are initially at rest, such that $R_p \gg 1$. At first, the effects of differential acceleration dominate and turbulence kinetic energy is created. Then, as viscous drag causes the particles to be swept along with the fluid, the velocity difference and the particle Reynolds number decrease, corresponding to a dampening of turbulent fluctuations. Since the amount of drag depends on the volume fraction of the particles, the turbulence level that is induced will also depend on this parameter.

These effects, however, address only a small fraction of the rich spectrum of dynamic processes that can occur in multifield turbulent flows. In our approach we discard the more conventional procedure of decomposing *velocities* and volume fractions and, instead, consider *momentum* and volume fractions as the primary variables to be conserved, decomposing these into their mean and fluctuating components. Such an approach allows us to derive two limiting fluid behaviors: diffusion (in the limit of strong momentum coupling between the particle and fluid fields), and wave-like interpenetration (in the weak-coupling limit). Our model is thus strongly analogous to the interpenetration of two different molecular species: diffusive when the mean free path is short, and wave-like when little or no coupling is present and the species transport as if each were expanding into a vacuum.

In addition, our model handles both ordered and disordered interpenetration of two phases as illustrated in Fig. 15. Other technical accomplishments include the resolution of mathematical ill-posedness of the multiphase flow equations, the emergence of a new closure principle (based on the constraint, with generalized Reynolds-stress expressions,

of exactly neutral stability for the mean-flow equations), and the development of practical modeling equations.

The modeling of turbulent flow with dispersed particles, droplets, or bubbles is of interest to a wide variety of scientific projects at the Laboratory. **For example, to** model the transport of dust and debris by volcanic eruptions, one must concentrate on the interactions between particulate and hot-gas flows. To improve the design of internal combustion engines, one needs an accurate prediction of both the combustion efficiency and the spatial distribution of heat generation, which, in turn, requires knowing the details of the mixing of fuel droplets and air. Although flow within the body's circulatory system is normally *not* turbulent, the transport of blood cells can be analyzed by using the equations for ordered two-field interpenetration. Other applications include modeling of the flow within nuclear reactors and the analysis of shock-wave motion in a gas that contains suspended particles.

Density Gradients. The second area we are currently striving to understand with transport modeling is turbulent mixing generated by strong density gradients that are sustained by large variations in thermal or material composition. Coupled with pressure gradients, such density gradients can lead to strongly contorted flow with intense vorticity near the steepest density variations. Again, the proper basis for deriving a generalized Reynolds stress lies in decomposing the momentum rather than the velocity.

Among the most important configurations to be studied are those for which adjacent materials—initially quiescent and of very different densities—are rapidly accelerated by a strong pressure gradient or heated by a sudden influx of radiation. The ensuing fluid instability (Richtmyer-Meshkov if the shock is going from heavy to light material, Rayleigh-Taylor for the opposite case (Fig. 7)) can act as a strong source for the turbulent mixing of the two materials.

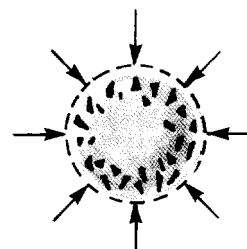
For example, consider an experiment in which a plane shock wave progresses down a closed cylindrical tube divided into two sections by a permeable membrane with air in the first section and helium in the second. As the shock passes from the dense to the less-dense gas, the air-helium interface is accelerated. Later, the interface is repeatedly decelerated by reflections from the rigid wall at the end of the tube. Interface instabilities lead to turbulent mixing of the two gases, and the initially sharp plane separating the gases becomes smeared and indistinct. **Our** work allows prediction of the average concentration across any strip of fluid taken normal to the nominal streaming direction and calculation of velocity and density profiles within the turbulent mixing zone.

Instabilities driven by density gradients are important to the study of the implosion dynamics of pellets used in inertial confinement fusion (Fig. 16). Radiation from a **high-**power laser initiates the implosion of an outer spherical capsule, creating a strong **shock** wave. This shock passes over the interface between the inner surface of the capsule and the enclosed gas, is reflected from the core, and returns to the interface where it induces Rayleigh-Taylor instability. The resultant mixing of gas and capsule in the central region of the pellet can, in many cases, reduce neutron yield.

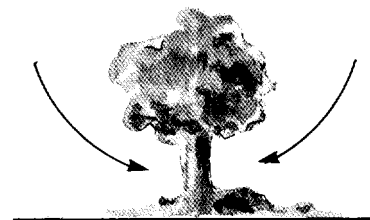
Another area of interest is the dynamics of fire plumes in the postulated circumstances of “nuclear winter.” Extreme heating of the ambient atmosphere produces up to four-fold expansions, resulting in a powerful updraft with intense turbulence.

CURRENT APPLICATIONS

Fig. 16. We are currently incorporating additional features in transport modeling so that more complex phenomena can be described adequately. An example is implosion of an inertial-confinement fusion capsule, during which two-phase turbulent interactions between the capsule and the hot fuel gases decrease the efficiency of the implosion. We also are investigating the density-driven turbulence that enhances mixing in fire plumes.



ICF Capsule Implosions



Nuclear Winter Fire Plumes

Supersonic Turbulence. Mach-number effects often can be ignored, but, in some cases (such as the high-Mach-number mitigation of a Kelvin-Helmholtz instability), such effects are significant. Thus, a third feature of our recent work has been to include the principal phenomena resulting from supersonic flow speeds. These effects arise across shock waves, in the shear layers behind Mach-reflection triple-shock intersections, and in the shear layers behind shock waves normal to a deformable wall.

An unexpected result of our work is the discovery that laminar instability theory (as sketched out in the section entitled “Turbulence Energy: Sources and Sinks”) is applicable to the study of supersonic turbulence. Despite the seeming inconsistency, this theory is providing highly relevant guidance to our early modeling efforts.

Concluding Remarks

A pertinent question is: What good is all this? Not only has our discussion illustrated several ways in which turbulence transport theory is heuristic or empirical, but the current large inventory of undetermined “universal” dimensionless parameters in its formulation is disturbing. Moreover, full expression of the theory is long and complicated, involving numerous coupled nonlinear partial differential equations. As a result, a transport calculation requires either costly numerical solutions or questionable approximations, or both.

What are the alternatives? There is no way to resolve turbulence in sufficient detail for numerical calculations based on turbulence transport theory to represent the effects of any but the simplest circumstances. Mixing-length theories and other point-functional approaches are hopelessly limited in their applicability. Fundamental approaches purporting to describe turbulence without empiricism are, in general, also restricted to highly idealized circumstances. Yet we are faced with the task of solving an endless variety of fluid-flow problems, a large fraction of which include significant turbulence effects. We need to supply answers to old questions and guidance for new developments in a meaningful way. At present, there seems to be no better approach to these challenging analytical tasks than that provided by turbulence transport theory.

Despite the shadows cast by these comments, the situation is actually far from gloomy. Turbulence transport theory seems to be functioning far better than we have any right to expect. There are at least four reasons for this good performance.

First, complex processes of nature often display a near universality in the collective effects that are of most interest. Just as gas molecules almost always have a nearly Maxwell-Boltzmann velocity distribution, it appears that turbulence tends toward a similar universality in its stochastic structure. The success of the few-variable (or collective, or moment) approach to turbulence modeling relies strongly on the validity of this contention. Although the extent to which universal behavior underlies most of the random processes of nature is currently a matter of intense scientific and philosophical discussion, much evidence supports the ubiquitous nature of this property. Perhaps, eventually, such universalities will help to successfully model such diverse instances as thoughts in a brain, activities of groups of organisms (such as mobs of people), and the dynamics of galaxies.

Next, turbulence transport modeling pays close attention to the binding constraints of real physics: conservation of mass, momentum, and energy, as well as rotational and

translational invariance. Such modeling also accounts for history-dependent variations lacking in many other turbulence theories.

We have also paid great care to physically meaningful closure modeling. Auxiliary derivations (like those of laminar instability analysis) combine with new formulations of mathematical restrictions (like that of precisely neutral mean-flow stability in the presence of generalized Reynolds-stress terms) to constrain our modeling procedures in the most physically meaningful manner possible at each stage of the development.

Finally, investigators throughout the world have made numerous comparisons with experiments, leading to corrections, improvements, and ultimately to considerable confidence in the broad applicability of the results.

Future research will concentrate on several significant aspects of the theory. Closure modeling, of course, continually needs strengthening, especially by first-principle techniques that decrease our reliance on empiricism. The numerical techniques need greater stability, accuracy, and efficiency for a host of larger and more complicated problems.

But the most intriguing challenge is how to incorporate new and different physical processes into our theories. For example, with dispersed-entity flow, we have scarcely begun to understand the effects of a spectrum of entity sizes or the deformation of individual entities (including their fragmentation and coalescence) or the modifications that arise when the entities become close-packed (as they do, for example, during deposition and scouring of river-bed sand). The dispersal of turbulence energy through acoustic or electromagnetic radiation is another interesting topic that needs considerable development. Deriving, testing, and applying the appropriate models will keep many investigators busy for a long time. ■

Further Reading

- B. J. Daly and F. H. Harlow. 1970. Transport equations in turbulence. *Physics of Fluids* 13: 2634–2649
- B. E. Launder and D. B. Spalding, 1974. The numerical computation of turbulent flows. *Computer Methods in Applied Mechanics and Engineering* 3: 269–289.
- C. J. Chen and C. P. Nikitopoulos. 1979. On the near field characteristics of axisymmetric turbulent buoyant jets in a uniform environment. *International Journal of Heat and Mass Transfer* 22: 245–255.
- D. Besnard and F. H. Harlow, 1985. Turbulence in two-field incompressible flow. Los Alamos National Laboratory report LA-10187–MS.
- F. H. Harlow, D. L. Sandoval, and H. M. Ruppel. 1986. Mathematical modeling of biological ensembles. Los Alamos National Laboratory report LA-10765–MS.
- D. Besnard, F. H. Harlow, and R. M. Rauenzahn. 1987. Conservation and transport properties of turbulence with large density gradients. Los Alamos National Laboratory report LA-10911–MS,
- D. Besnard and F. H. Harlow. Turbulence in multiphase flow. Submitted for publication in *International Journal of Multiphase Flow*.

Authors

Didier Besnard is a frequent visitor to Los Alamos from the Commissariats a l'Energie Atomique in France. He is the recipient of several advanced degrees in the fields of applied mathematics and engineering and has been employed since 1979 at the Centre d'Etudes de Limeil-Valenton, near Paris, where he is head of the Groupe Interaction et Turbulence. He is especially active in the analytical and numerical solution of problems in plasma physics and the high-speed dynamics of compressible materials. At Los Alamos he has worked in the Center for Nonlinear Studies and been a Visiting Scientist in the Theoretical Fluid Dynamics Group, collaborating in the development of turbulence transport theories, especially for multiphase flows and fluids with large density variations. An avid rock climber, hiker, and skier, he enjoys frequent excursions to the backwoods areas of both New Mexico and the French Alps. His wife, Anne, and daughter, Gaelle, join him in being a truly international family, spending at least a month in New Mexico each summer.

Francis H. Harlow came to Los Alamos in September 1953 after receiving his Ph.D. from the University of Washington and has been a physicist in the Theoretical Division during his entire employment at the Laboratory. Special interests include fluid dynamics, heat transfer, and the numerical solution of continuum dynamics problems. He was Leader of the Fluid Dynamics Group for fourteen years and became a Laboratory Fellow in 1981. His extensive publications describe a variety of new techniques for solving fluid flow problems and discuss the basic physics and the application to practical problems. Northern New Mexico has served as a strong stimulus to his collateral activities in paleontology, archeology, and painting. Writings include one book on fossil brachiopods and four on the Pueblo Indian pottery of the early historic period. His paintings have been the subject of several one-man shows and are included in hundreds of collections throughout the United States.



Left to right: Norman L. Johnson, Rick Rauenzahn, Francis H. Harlow, Jonathan Wolfe, and Didier Besnard.

Norman L. Johnson came to Los Alamos in the summer of 1981 as a graduate student working on cavity radiation and the numerical solution of highly nonlinear equations within a thermal-fluid finite element code. In the spring of 1983, he completed his Ph.D. in free Lagrangian methods and kinetic theory for viscoelastic flows at the University of Wisconsin in Madison. He returned to Los Alamos as a postdoctorate and developed an interest in modeling the complex physics of hypervelocity impact phenomena. Concurrently with his stay at Los Alamos, he held a position at the National Bureau of Standards in Boulder, Colorado, working on facilitated transport across membranes. In 1985 he became a permanent staff member in the Theoretical Fluid Dynamics Group and is currently working on the development of a local intense energy source and on numerical methods for flows with high distortions. Special interests include impact phenomena and the rheology of viscoelastic fluids and suspensions. In off hours he is currently learning how to juggle, as well as continuing his enjoyment of modern dance and the Japanese language and culture.

Rick Rauenzahn came to Los Alamos in 1982 as a graduate student in the Earth and Space Sciences Division to research the fundamentals of thermal spallation drilling. Prior to this, Rick had received his B.S. from Lehigh University in 1979 and his S.M. from MIT in 1980, both in chemical engi-

neering. Two one-year stints in the chemical industry prepared him to enter MIT once again, and, in 1986, after doing thesis work at the Laboratory, he received his Ph. D. in Chemical Engineering. Since then, he has been in the Theoretical Fluid Dynamics Group, working on the fundamentals of turbulence modeling, mixing at interfaces, and two-dimensional code development.

Jonathan Wolfe is an undergraduate student in the Mechanical Engineering Department at the University of New Mexico, participating in the Cooperative Education Program with Los Alamos. In a cross-country pursuit of his education, Jon came to New Mexico in 1983 and to Los Alamos soon afterwards. Working for the Earth and Space Sciences Division, he contributed to the development of innovative computational techniques for the solution of large, sparse matrix systems, and worked as a field engineer ("grunt") at the Fenton Hill geothermal test site. More recently, he has been a member of the Theoretical Fluid Dynamics Group, collaborating in the numerical investigation of problems in turbulence and multiphase flow. Jon has fallen in love with the New Mexico outdoors, and spends lots of time windsurfing, motorcycling, and playing ultimate frisbee, despite the threat of impending graduation and responsibility.